# Raman study of hydrogen-saturated silica glass

K.P. Meletov[*], V.S. Efimchenko

Institute of Solid State Physics, Russian Academy of Sciences, Chernogolovka, Moscow region, 142432 Russia

HIGHLIGHTS

- Raman spectra of saturated H_2 solution in silica were measured for the first time.
- The rotational mode frequency decreases with the amount of dissolved H_2.
- The vibration mode frequency increases with the amount of dissolved H_2.
- The H_2/D_2 isotopic effect agrees quantitatively with theory of diatomic molecule.
- The intensity of hydrogen phonon bands exponentially decreases with annealing time.

GRAPHICAL ABSTRACT
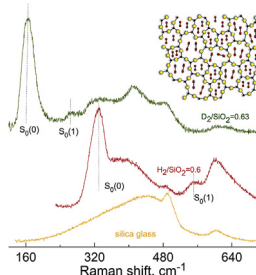
ABSTRACT

The Raman spectra of saturated solid solutions of hydrogen and deuterium in silica glass, SiO_2-$0.6H_2$ and SiO_2-$0.63D_2$, have been measured for the first time at liquid nitrogen temperature. The comparative analysis of H_2 phonon modes in solid solution of hydrogen in silica glass and those of hydrogen gas shows a decrease in the frequency of rotational modes contrary to an increase in the H−H stretching vibration mode frequency. Hydrogen rotational modes, overlapped with the phonon modes of silica glass, strengthen at an elevated temperature, while the phonon modes of silica glass soften. The isotopic substitution of hydrogen by deuterium leads to a decrease in the stretching vibration mode frequency proportionally to the square root of D_2/H_2 mass ratio, whereas rotational mode frequencies decrease as a ratio of D_2 to H_2 inertia moments. The intensity of H_2 phonon modes gradually decreases upon the heating of hydrogen-saturated silica glass along with the evolving of dissolved hydrogen.

© 2021 Hydrogen Energy Publications LLC. Published by Elsevier Ltd. All rights reserved.

---

* Corresponding author.
    E-mail address: meletovk@yandex.ru (K.P. Meletov).

Introduction

A search for hydrogen storage materials has a long and abundant history [1]. Besides gas and liquid storage, the storing of hydrogen into a solid is a good alternative since it is possible to contain more hydrogen per unit volume [2]. Considerable solubility of hydrogen in metals, intermetallic compounds, carbon nanostructures, clathrates of various gases and ice hydrates is well described in literature [3—7]. The absorption rate of hydrogen in atomic or molecular form, total absorbed amount, the availability of absorbing and releasing way, as well as the prevalence of potentially useable hydrogen storage materials play an important role in applications. In this regard, a variety of pure and doped silicates is of considerable interest for their possible use as hydrogen storage materials.

In 1976, C. Hartwig carried out the first successful experiments on the dissolution of molecular hydrogen and deuterium in silica glass [8]. Certain solubility was observed at a temperature of $90°C$ and hydrogen gas pressure between 6.6 and 84.9 MPa. The Raman tests of hydrogenated silica glass identified the H−H stretching vibration mode growing in intensity with an increase in the hydrogen concentration to a maximum of $\sim 0.06 H_2/SiO_2$ at 84.9 MPa. The saturated solid solutions of hydrogen in silica glass were obtained in 2013; rather a high solubility of $X = H_2/SiO_2 = 0.16$ was found at a pressure of 0.6 GPa and $250°C$, which drastically increases to $X = 0.53$ at a pressure of 7.5 GPa [9]. The saturated solid solutions of hydrogen in silica glass are metastable and, after synthesis, were stored in liquid nitrogen to prevent hydrogen losses under ambient conditions. Thereafter, the solid solutions of hydrogen in some other doped silicates were prepared under the similar conditions of hydrogen pressure and temperature. The temperature range of their stability and the amount of dissolved hydrogen were examined by hot extraction into pre-evacuated volume, whereas changes in the structure of a silicate matrix upon hydrogenation were studied by X-ray diffraction near liquid nitrogen temperature [10—13]. However, these experiments do not provide any information about the properties of dissolved hydrogen, like the interaction of hydrogen with a silica glass matrix and changes in the phonon spectra of hydrogen and silica glass. In this regard, Raman spectroscopy is more useful, which may clarify the chemical state of dissolved hydrogen and its interaction with a silica glass matrix. Raman spectroscopy provides a powerful tool for the study of dissolved hydrogen and the comparison of its properties with those of pure hydrogen under ambient and/or extreme conditions.

The Raman spectra of liquid hydrogen were first measured in 1929, soon after the discovery of the Raman scattering effect and the development of technology for condensation of nitrogen, hydrogen, and helium gases [14]. The measurements of hydrogen Raman spectra in liquid and solid states were carried out before the development of lasers using the intense lines of a mercury lamp as a source of monochromatic light [14—16]. The phonon modes of hydrogen molecules show minor changes in the frequencies and bandwidths during gas − liquid - crystal transitions at ambient pressure and low temperatures. Hydrogen diatomic molecules may be in two different states, with parallel (ortho) and anti-parallel (para) nuclear spins, which differ in the frequencies of rotational and stretching vibration modes. The population of ortho- and para-states depends on temperature; at ambient temperature, ortho-hydrogen predominates, whereas at liquid hydrogen temperature para-hydrogen prevails due to ortho-para conversion.

After the development of the diamond anvil technique, a great interest appeared in the experimental studies of hydrogen at an extremely high pressure. A search for a metallic state in highly compressed hydrogen became an exciting goal for many years in view of predictions for high-temperature superconductivity in this material [17]. The progress in the generation of unprecedented high static pressure stimulated structural and Raman studies of hydrogen under extreme conditions. Although metallic hydrogen has not been found until today at pressures as high as 300 GPa, these studies provided important knowledge of the properties of hydrogen at ultrahigh pressures that refer to the stability of a hydrogen molecule and behavior of rotational and stretching vibration modes [18—20]. Finally, Raman spectroscopy is widely used in the studies of ice clathrates, which were synthesized by the saturation of ice with hydrogen or deuterium at a temperature from $-10°C$ to $-20°C$ and gas pressure from 80 to 200 MPa with the subsequent quenching of samples in liquid nitrogen [21—23]. These studies revealed the regularities in the phonon frequencies of molecular hydrogen adsorbed in ice pores of various sizes. In this way, the kinetics of hydrogen dissolution under various conditions of synthesis and hydrogen desorption at an elevated temperature were studied.

In the present work, we report the results of the Raman study of saturated solid solutions of hydrogen and deuterium in silica glass, synthesized at a pressure from 2.8 to 7.5 GPa and a temperature of $250°C$. For the first time, the Raman spectra of saturated solid solutions of hydrogen and deuterium in silica glass have been measured in the range of $90-4300$ cm^{-1} at near liquid nitrogen temperature and ambient pressure. The phonon modes of dissolved hydrogen change markedly as compared with those of hydrogen gas; the frequencies of rotational modes, overlapped with the phonon spectrum of silica glass, decrease, while the frequency of the H−H stretching vibration mode increases. The spectra of deuterated silica glass show a pronounced isotopic effect that differs for rotational and stretching vibration modes. The amount of dissolved hydrogen strongly affects the intensity, frequency, and bandwidth of its phonon modes, which allows studying hydrogen desorption kinetics upon the annealing of samples at an elevated temperature.

Experimental

The samples of OH-Vitreosil silica glass purchased from Sigma−Aldrich with 99.9 wt % purity contained <0.01 wt% metals and <0.06 wt% OH$^-$ impurities. The initial samples were annealed before the hydrogenation for 4 h at 800 °C to eliminate hydroxyls and water. The hydrogenation was carried out in a toroid-type high-pressure apparatus [24] using AlH$_3$ [25] or NH$_3$BH$_3$ [26] as an internal hydrogen source. The high-pressure cell was made of Teflon; a Pd foil separated the silica glass from the hydrogen source. To evolve hydrogen, AlH$_3$ or NH$_3$BH$_3$ was decomposed at P = 1.5 GPa by heating to

T = 250 °C. After that, the pressure was increased, and the silica glass was exposed to an H_2 atmosphere at P = 7.5 GPa and T = 250 °C for 24 h and, finally, quenched to −196 °C to prevent hydrogen losses in the course of pressure release. The molar ratio X = $H_2/f.u.$ of the samples was determined with an accuracy of 3% by hot extraction into pre-evacuated volume [27]. The hydrogenated silica glass samples were stored in a liquid nitrogen vessel and studied further by Raman spectroscopy and X-ray diffraction at T = 85 K. The Raman spectra were recorded in back-scattering geometry using a micro-Raman setup comprised of an Acton SpectraPro-2500i spectrograph and a CCD Pixis2K. The 532-nm line of a single-mode YAG CW diode-pumped laser was focused on the sample by an Olympus BX51 microscope using 50 × objective. The spatial resolution was ~2 μm, while the spectral resolution varied between 2.3 and 4.1 cm^{-1}. The laser line was suppressed by an edge filter with OD = 6 and bandwidth of ~100 cm^{-1}, while the beam intensity before the sample was ~5 mW. The Raman spectra at various temperatures were taken using a self-made nitrogen cryostat with cold loading of samples without intermediate warming. The cryostat equipped with a temperature controller and resistive heater provided temperature control in the region of 83–250 K with an accuracy of ±0.4 K [28].

Results

Fig. 1 depicts the Raman spectra of as-prepared solid solution of hydrogen in silica glass SiO_2-0.58H_2 (closed circles) and after its annealing at room temperature for 90 min (open circles) in the energy region of 250–4300 cm^{-1} and ~85 K. The solid line in the figure depicts the Raman spectrum of hydrogen gas at

room temperature and a pressure of ~0.5 MPa. The last spectrum contains narrow bands of $S_0(0)$ and $S_0(1)$ rotational modes with frequencies of 354 и 587 cm^{-1}, corresponding to para- and ortho-hydrogen, respectively. At high energy, it contains narrow bands of the H-H stretching vibration modes $Q_1(1)$ and $Q_1(0)$ with frequencies of 4155.5 and 4162.5 cm^{-1}, which also correspond to ortho- and para-hydrogen, respectively. Asterisks indicate stretching vibration modes $Q_1(2)$ and $Q_1(3)$ that refer to poorly populated rotational states with J = 2 and J = 3. Their intensity drops at low temperature along with a decrease in the population of rotational states. The frequencies of the rotational and stretching vibration phonon modes of gaseous hydrogen are the same as those reported earlier [22,25]. The phonon spectrum of the annealed SiO_2-0.58H_2 sample coincides with that of pristine silica glass [29], which differs markedly from the spectrum of the as-prepared sample. The difference relates firstly to a wide intense band with a frequency of ~4190 cm^{-1} that appears in the high-energy region. Secondly, in the low-energy region two bands appear with frequencies of ~328 cm^{-1} and ~549 cm^{-1}, overlapped with the phonon spectrum of silica glass. The intensities of all these bands gradually decrease upon the heating of samples and loss of hydrogen, which indicates that they refer to the phonon modes of dissolved hydrogen molecules. The band at ~4190 cm^{-1} corresponds to the $Q_1(0)$ stretching vibration mode of a hydrogen molecule, whereas the bands at ~328 cm^{-1} and ~549 cm^1 correspond to $S_0(0)$ and $S_0(1)$ rotational modes, respectively. The phonon bands of hydrogen in hydrogenated silica glass are very broad: their bandwidth is ~45 cm^{-1} for the stretching vibration mode and ~35 cm^{-1} for the rotational mode. On the contrary, the phonon modes of gaseous hydrogen are very narrow because their bandwidth of ~3 cm^{-1} in the Raman spectra is actually the
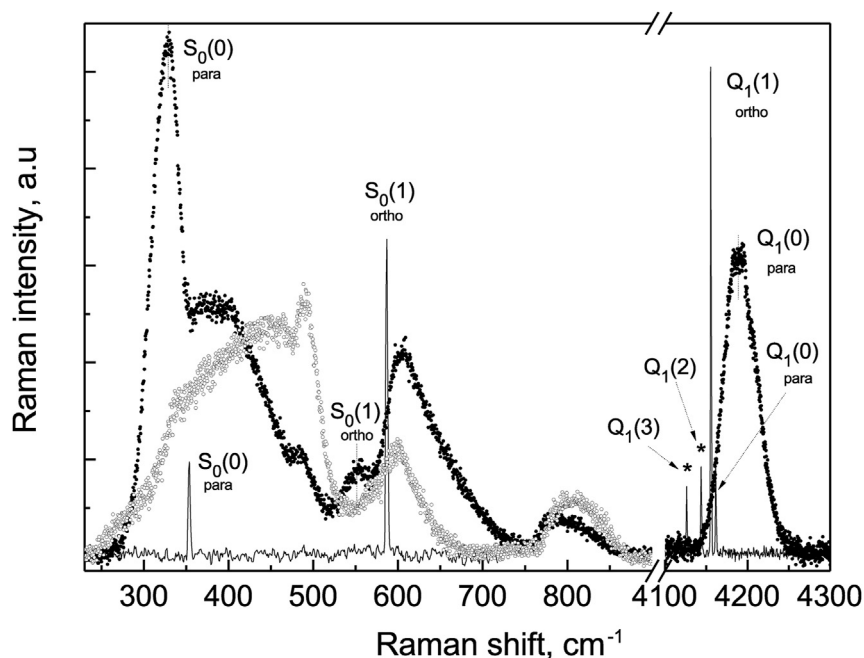
Fig. 1 – Raman spectrum of hydrogenated SiO2-0.58H_2 silica glass in the energy region of 250–4300 cm^{-1} and at 85 К (solid symbols), Raman spectrum of the same sample after 90-min annealing at room temperature (open symbols), and Raman spectrum of gaseous hydrogen at room temperate and 5 bar (solid line).

width of the spectrometer slit. The frequencies of the phonon modes of dissolved hydrogen differ from those of hydrogen gas: the rotational modes shift towards lower energies by ~20 cm^{-1}, while the stretching vibration mode shifts up in energy by ~30 cm^{-1}. In addition, the relative intensities of para- and ortho-hydrogen modes in solid solution of hydrogen in silica glass and hydrogen gas differ because para-hydrogen prevails in samples quenched at liquid nitrogen temperature due to ortho-para conversion [23]. The overlapping of hydrogen rotational modes with the phonon spectrum of silica glass causes some problems with their unambiguous assignment. The identification of the intense $S_0(0)$ mode at the low-energy edge of the phonon spectrum is undoubted, while the assignment of weak $S_0(1)$ band requires additional argumentation, which will be given later in the text.

Fig. 2 depicts the Raman spectra of hydrogenated (closed circles) and deuterated (open circles) silica glass samples with SiO_2-$0.6H_2$ and SiO_2-$0.63D_2$ compositions, measured at ~85 K in the frequency range of $90 \div 4300$ cm^{-1}. The substitution of hydrogen by deuterium leads to the isotopic shift of the stretching vibration mode, which shifts towards lower energies from 4190 cm^{-1} in hydrogenated silica glass to 3016 cm^{-1} in deuterated silica glass. The frequency ratio for this mode of ~1.389 is less than the classical value for an isotopic shift in harmonic approximation $(M^D/M^H)^{1/2} = 1.414$. Rather a large difference is associated with quantum effects at low temperatures, which are manifested due to a very high Debye temperature of hydrogen of ~1700 K [30]. Concerning the rotational modes, the $S_0(0)$ mode frequency of ~328 cm^{-1} in SiO_2-$0.63H_2$ decreases to ~165 cm^{-1} in SiO_2-$0.63D_2$. Thus, the frequency ratio of ~1.988 for this band is closer to its theoretical value in harmonic approximation, which is equal to the ratio of the inertia moments of D_2 and H_2 molecules $I^D/I^H = 2$ [31]. The spectrum of deuterated silica glass contains also a weak shoulder near 260-280 cm^{-1}, which may be assigned to the $S_0(1)$

mode of deuterium because its frequency is approximately half the hydrogen $S_0(1)$ mode frequency in hydride. Additionally, the Raman spectrum of deuterated silica glass contains a weak band near the $Q_1(0)$ stretching vibration mode of deuterium which refers to the traces of water, as well as a weak band of ~328 cm^{-1} corresponding to the $S_0(0)$ mode of small hydrogen contaminant.

Fig. 3 shows the temperature dependence of the frequencies of hydrogen phonon modes in hydrogenated silica glass SiO_2-$0.6H_2$ sample and several phonon modes of a silica glass matrix. The right panel shows the Raman spectra of pristine silica glass (lower spectrum) and SiO_2-$0.6H_2$ sample (upper spectrum). The inset in the right panel shows the fitting of bands in the SiO_2-$0.6H_2$ phonon spectrum by the Voigt profile. The left panel illustrates the temperature dependence of the relative phonon frequencies, Ω_T/Ω_{80}, defined during the Raman measurements of pristine silica glass and hydrogenated silica glass at various temperatures. The spectra were measured in the temperature range of $80 \div 185$ K using a nitrogen cryostat with cold loading of samples and a temperature controller [28]. The bottom part of the left panel shows the dependence of several phonon modes of glass on the temperature, whereas the upper part depicts the temperature dependence for hydrogen phonon $S_0(0)$, $S_0(1)$, and $Q_1(0)$ modes. The frequencies of glass phonon modes decrease with an increase in the temperature; this behavior of phonon modes is related to the anharmonicity of vibrations and thermal expansion. Otherwise, when the thermal expansion is small, the phonon frequencies almost do not change. This is a case of pristine silica glass, which has almost zero thermal expansion in the temperature range under study. Contrary to glass vibrations, the frequencies of rotational $S_0(0)$ and $S_0(1)$ modes of hydrogen increase with temperature; different temperature behavior confirms the correct identification of these modes performed above. At the
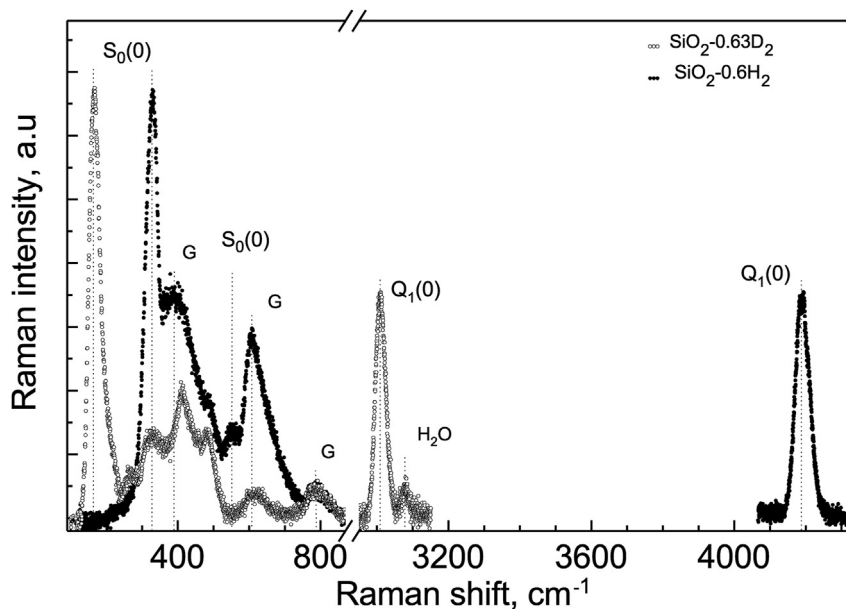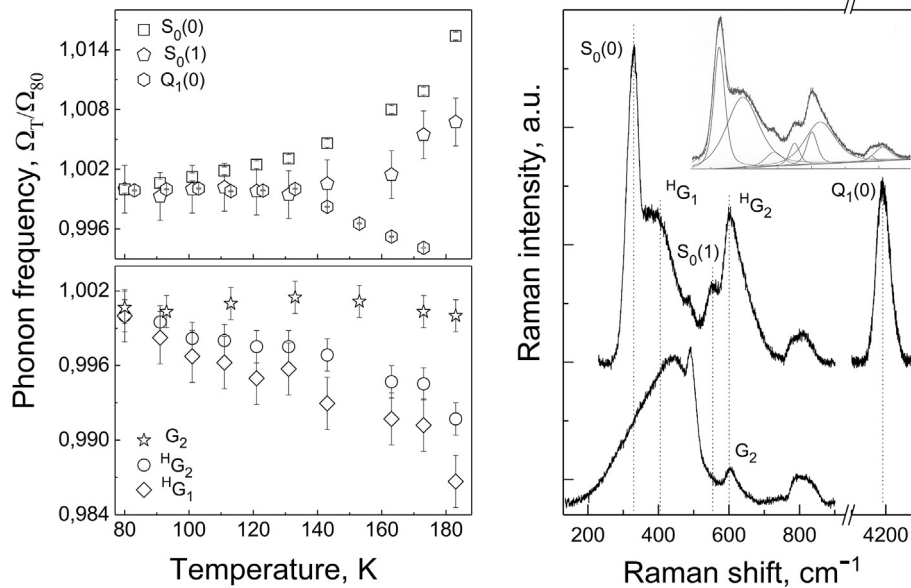

Fig. 2 — Raman spectra of hydrogenated SiO_2-$0.6H_2$ silica glass sample (solid symbols) and deuterated SiO_2-$0.63D_2$ silica glass sample (open symbols) measured in the energy region of $90-4300$ cm^{-1} at 85 K.

Fig. 3 — Left panel - Temperature dependence of the phonon frequencies of dissolved hydrogen and silica glass matrix. Right panel - Raman spectra of hydrogenated silica glass sample SiO$_2$-0.6H$_2$ (upper spectrum) and pristine silica glass (lower spectrum). The inset — fitting of the phonon bands by the Voigt function.

same time, the frequency of the $Q_1(0)$ stretching vibration mode decreases when the temperature increases. The changes in hydrogen phonon frequencies are irreversible with temperature; they refer most likely to hydrogen losses upon heating. This assumption is consistent with the similar changes in the frequencies of hydrogen phonon modes observed in the Raman spectra of hydrogenated silica glass samples with different amounts of dissolved hydrogen. Fig. 4 shows the Raman spectra of two different hydrogenated silica glass samples synthesized at hydrogen pressures of 2.8 GPa and 7.5 GPa and a temperature of 250 °C, which

contain X = 0.39 and X = 0.69 hydrogen, respectively. The left panel represents the Raman spectra of hydrogenated silica glass samples near the $S_0(0)$ rotational mode at 85 K with hydrogen content X = 0.39 (closed circles) and X = 0.69 (open circles). The right panel shows the spectra near the $Q_1(0)$ stretching vibration mode. An increase in the dissolved hydrogen leads to a decrease in the rotational mode frequency and an increase in the frequency of the stretching vibration mode.

The frequency and intensity of hydrogen phonon bands in saturated solid solutions of hydrogen in silica glass change due
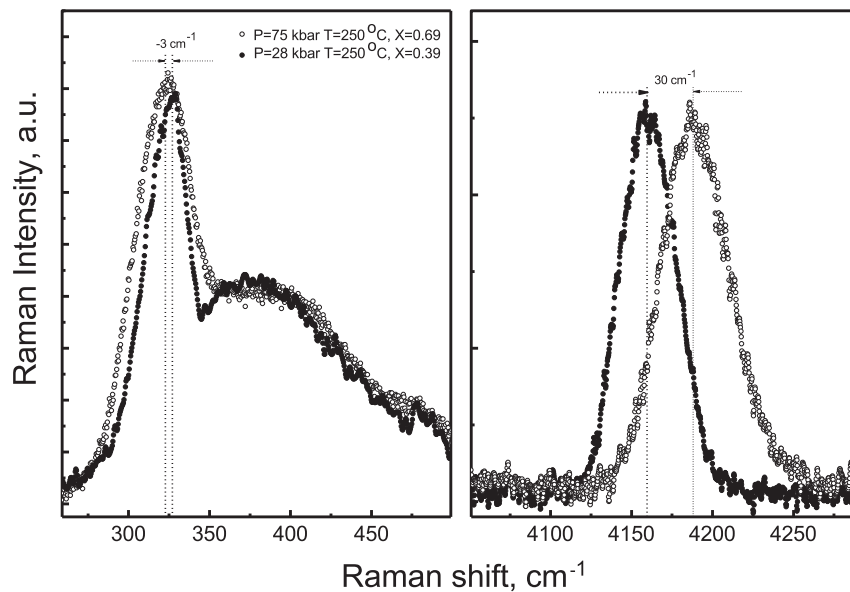
Fig. 4 — Raman spectra of two different solid solutions of hydrogen in silica glass at 85 К. Solid symbols - H$_2$/SiO2 = 0.39, open symbols — H$_2$/SiO2 = 0.69. Left panel - S$_0$(0) mode, right panel - Q$_1$(0) mode.

to hydrogen losses upon the heating of samples. Fig. 5 shows the variations of the Raman spectra of hydrogenated silica glass recorded in the frequency range of 250–900 cm^{-1} upon the annealing of samples at 173 к for 8, 43, and 123 min. The intensity of hydrogen rotational modes decreases with an increase in the annealing time; the magnitude of changes associated with the ratio of the summarized intensity of rotational bands to the intensity of the phonon bands of silica glass grows up. Note that the latter does not change upon annealing and serves as an intensity scale. The dependence of hydrogen content on the annealing time associated with the relative intensity of rotational modes I_H to the intensity of silica glass modes I_G is shown with closed circles; it is well described by the exponential decay function 27∗exp(-t/26.2)+35 (dashed line). The primary content of dissolved hydrogen X = 0.62 determined by hot extraction was used for the calibration of hydrogen rotational mode intensity to the intensity of silica glass modes as 62%. The exponential decay time constant is ~26 min, while the process saturates at large annealing time showing residual hydrogen content of ~35%. The Raman spectra recorded in backscattering geometry show the phonon spectrum on the surface of samples. Thus, a decrease in the intensity of hydrogen bands shows a decrease in the hydrogen concentration on the surface of a sample, while diffusion of hydrogen from the depth of the sample leads to its partial replenishment. At a certain stage of annealing, the amount of hydrogen released from the sample surface becomes equal to the appropriate amount of hydrogen incoming from the bulk. In our opinion, these steady-state conditions determine residual hydrogen content as measured by Raman spectroscopy. The inset in the figure shows the content of desorbed hydrogen for SiO$_2$-0.58H$_2$ during hot extraction. The hot extraction curve

was obtained by continuous heating of the sample in a closed pre-evacuated ampoule from −190 °C to 500 °C at a rate of ~15° per minute. Desorption is very small in the temperature range up to −100 °C, it intensifies at a temperature of −50 °C, and becomes violent near 0 °C. The determination of hydrogen amount in this way is applicable to all types of hydrogenated solids; however, the study of desorption kinetics requires a different approach. The variation of the relative intensity of hydrogen phonon modes upon annealing at different temperatures provides valuable information on the kinetics of hydrogen desorption that allows specifying the activation energy of hydrogen release.

Discussion

The dissolution of molecular hydrogen in silica glass modifies its phonon spectrum. The intensity and frequency of new appeared hydrogen phonon modes change with an increase in the adsorbed hydrogen amount. The phonon spectrum of a free hydrogen molecule consists of rotational modes associated with rotations of a diatomic molecule, and of stretching vibration of hydrogen atoms along the bond direction. The energy of rotational phonon modes is:

$$E = B_0 \cdot J \cdot (J + 1) \qquad (1)$$

where $B_0 = h/(8\pi^2 Ic)$ − is the rotational constant, $J = 0, 1, 2, ...$ − is the rotational quantum number, $I = \mu R^2$ − is the moment of inertia of a diatomic molecule (μ − is the reduced mass, R − is the distance between atomic nuclei), h–is the Planck constant, c − is the speed of light.
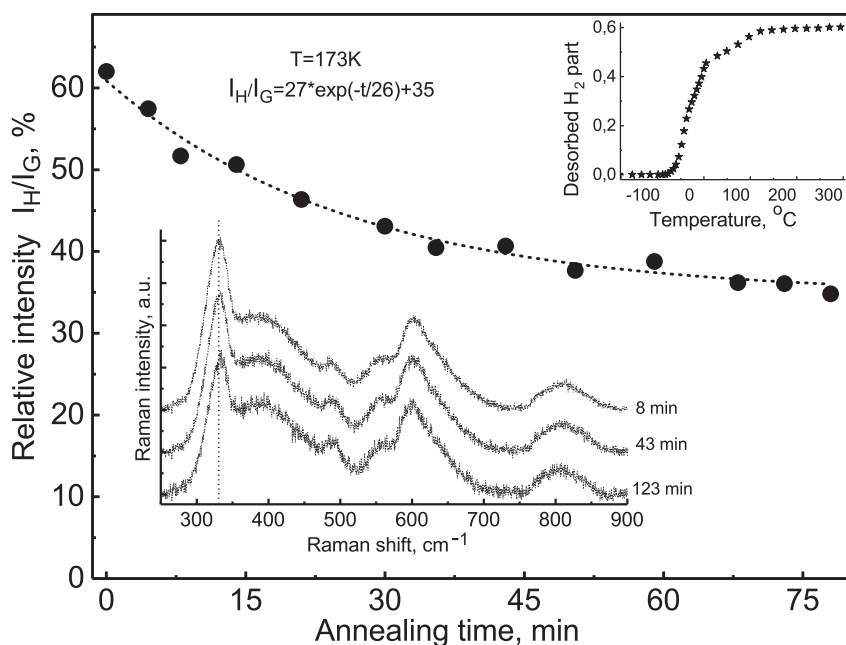
Fig. 5 − Raman spectra of saturated solid solutions of hydrogen in silica glass in the energy region of 250–900 cm^{-1} during annealing at 173 к after 8, 43, and 123 min. Closed symbols - dependence of hydrogen content (relative Raman intensities of hydrogen and silica glass modes I$_H$/I$_G$) on the annealing time, dotted line − fitting of the experiment by exponential decay function. Inset − hot desorption of hydrogen under the continuous heating of hydrogenated silica glass sample.

The energy of the stretching vibrations is:

$$E = (n + 1/2) \cdot h\nu \tag{2}$$

where $\nu = (1/2\pi) \cdot (\kappa/\mu)^{1/2}$, n-is the vibration quantum number, κ-is the force constant, μ-is the reduced mass [31].

The rotational $S_0(0)$ mode of para-hydrogen corresponds to the transition between $J = 0$ and $J = 2$ states with the energy $6B_0$, whereas the rotational $S_0(1)$ mode of ortho-hydrogen corresponds to the transition between $J = 1$ and $J = 3$ states with the energy $10B_0$. For gaseous hydrogen under ambient conditions, $B_0 = 59.2$ cm^{-1} for the $S_0(0)$ mode and $B_0 = 58.7$ cm^{-1} for the $S_0(1)$ mode [15]. Thus, a change in the nuclear spin of a hydrogen molecule affects the rotational constant B_0. The frequencies of rotational modes increase by 1.5 cm^{-1} due to the enhancement of intermolecular interaction upon the condensation of hydrogen, whereas the compression of liquid hydrogen to 4 GPa results in a further increase by ~5 cm^{-1} [15,18]. An increase in the intermolecular interaction upon the solidification of hydrogen above 5.5 GPa leads to significant broadening of rotational modes and results in their degradation with a further increase in the pressure [18]. The frequency of the $Q_1(1)$ stretching vibration mode increases with pressure up to ~30 GPa, while a further increase in the pressure results in its decrease [18]. The contraction of the H-H molecular bond at high pressure leads to an increase in the elastic constant and frequency of the stretching vibration mode $\nu = (1/2\pi) \cdot (\kappa/\mu)^{1/2}$. At the same time, the inertia moment of a molecule decreases, and the rotational constant $B_0 = h/(8\pi^2 I c)$, as well as the frequency of the rotational mode, increases. The softening of the stretching vibration mode above 30 GPa refers to the so-called centralization of the H-H bond caused by the enhanced interaction between hydrogen atoms of neighboring H$_2$ molecules resulting in some expansion of the intra-molecular bond. The inhibition of molecular rotation in solid hydrogen causes the broadening of rotational modes, and, according to estimates, the rotation is predicted to cease at ~37.5 GPa that, in fact, occurs earlier [18,32]. The narrowing of the $Q_1(1)$ stretching vibration band, observed at a pressure P > 5.5 GPa, also refers to the inhibition of hydrogen molecule rotations after solidification [18].

It is interesting to compare the behavior of the rotational and stretching vibration modes of liquid hydrogen at high pressure with that of the rotational and stretching vibration modes of hydrogen dissolved under pressure in silica glass and clathrates. In ice clathrates synthesized at low hydrogen pressure, the $S_0(1)$, $S_0(0)$, and $Q_1(1)$ mode frequencies decrease compared to the phonon frequencies of a free hydrogen molecule. In this case, the lowest phonon frequency is observed for single hydrogen molecules embedded in the largest voids in the crystal structure of clathrate [21—23]. As the void size decreases, either two, three, or four hydrogen molecules fill large voids, the frequencies of rotational and stretching vibration modes gradually increase; however, they are always less than the corresponding frequencies of gaseous hydrogen [33]. The similar behavior was observed for the $Q_1(1)$ mode in diluted solid solutions of hydrogen in silica glass with a small amount of hydrogen obtained by Hartwig at relatively low hydrogen pressure [8]. Unfortunately, no data on the rotational $S_0(0)$ and $S_0(1)$ modes were presented in Ref. [8] to compare them with those of ice clathrates. Nevertheless, these modes appear in the Raman spectra of germanosilicate optical fibers filled with hydrogen at relative low pressure of ~170 MPa [34]. As in the case of ice clathrates, in germanosilicate optical fibers both rotational $S_0(0)$ and $S_0(1)$ modes, as well as the stretching vibration $Q_1(1)$ mode, are shifted towards low energies [34]. According to Ref. [23], a decrease in the hydrogen mode frequencies in ice clathrates is related to the softening of the covalent bond due to the van der Waals attractive interaction between water and hydrogen molecules in the voids of clathrate. The expansion of the H-H bonds leads to an increase in the inertia moment and a decrease in the elastic constant of the molecule resulting in the softening of both rotational and stretching vibration modes. Pimentel and Charles [35] explained this trend of frequency change using the «loose cage − tight cage» model. In this model, the shift of the vibration mode frequency of an encaged molecule relative to a free molecule $\Delta\omega_{n,0}$ is determined by the first and second derivatives U' and U'' of the solute-solvent interaction potential with respect to the internal stretching coordinate of the encaged molecule:

$$\Delta\omega_{n,0} = (nB_e /hc\omega_e)^* < U'' \text{-} 3AU' >_{\tau 0} \tag{3}$$

where $< >_{\tau 0}$ is the statistical average of all configurations (τ) of the solute in the ground state, and n, B_e, h, c, ω_e, and A represent the number of the excited vibrational state, the equilibrium rotational constant, Plank's constant, the speed of light, the equilibrium vibrational frequency, and the anharmonicity constant, respectively. The term in (3) associated with U'' arises from a change in the harmonic force constant due to the intermolecular interaction, and the term associated with U' arises from a shift in the equilibrium displacement and is important when the vibration is anharmonic. Depending on the solute-solvent interaction potential, both negative and positive frequency shifts are possible.

The changes in the frequencies of hydrogen phonon modes in saturated solid solutions of hydrogen in silica glass differ from those of ice clathrates, as well as from pressure-induced changes in liquid hydrogen. The frequencies of hydrogen rotational modes in hydrogenated silica glass decrease contrary to an increase in the stretching vibration mode frequency, while the bandwidths of all modes increase markedly. In this regard, the saturated solid solutions of hydrogen in silica glass obtained at high hydrogen pressure differ from those obtained at relatively low hydrogen pressure, such as ice clathrates [23], diluted solid solutions of hydrogen in silica glass [8], or germanosilicate optical fibers filled with hydrogen at relative low pressure of ~170 MPa [34] with a small amount of hydrogen. In ice hydrates C_1 and C_2, in which molecules at relatively high hydrogen pressure are embedded in the interstitial positions of the crystal lattice of ice II and Ic, respectively, the frequency of the $Q_1(1)$ mode increases markedly [36]. Moreover, when ice hydrate C_1 transforms to ice hydrate C_2 at a pressure of ~4 GPa, the concentration of dissolved hydrogen $X = H_2/H_2O$ increases from $X \approx 0.17$ to $X \approx 1$, and the frequency of the stretching vibration mode increases additionally by ~20 cm^1 [36]. Thus, an increase in the content of dissolved hydrogen typical of saturated solid solutions of hydrogen in silica glass results in a significant shift of the stretching

vibration mode towards higher energies. Unfortunately, there are no data on rotational modes in [36] to compare them with those in hydrogenated silica glass. Obviously, the frequency of the stretching vibration mode increases due to the contraction of the H–H bond caused by the pressure-enhanced interaction of hydrogen molecules in saturated solid solutions of hydrogen in silica glass. At the same time, the H-H bond length and the moment of inertia decrease, therefore, the frequency of rotational modes should increase. Such behavior is shown by rotational and stretching vibration modes in liquid hydrogen at high pressure before its solidification [18]. In contrast, an increase in the hydrogen content in saturated solid solutions of hydrogen in silica glass results in a decrease in the rotational mode frequency. We believe that hydrogen in the voids of silica glass is in the gaseous state at high pressure. Thus, the free rotation of hydrogen molecules under these conditions may be somewhat inhibited due to the interaction with the "fixed" atoms of silica glass at the void boundaries. Intuitively, it reminds reducing of mechanical top rotation due to the friction of the top axes against the surface. This is consistent in part with the experimental results [18] related to the strong broadening of rotational modes near hydrogen solidification followed by their degradation under a further increase in the pressure. Thereby, the intermolecular interaction at high pressure in hydrogen gas within the voids of silica glass decreases the frequency of rotational modes, the magnitude of which exceeds, however, an increase in the frequency caused by the shortening of the H-H bond.

Conclusions

The Raman spectra of saturated solid solutions of hydrogen in silica glass prepared at hydrogen pressure of 7.5 GPa and 250°C show a large amount of dissolved molecular hydrogen. In the phonon spectrum of hydrogenated silica glass, the rotational and stretching vibration modes of hydrogen appear that grow in the intensity at higher hydrogen concentration and change somewhat the phonon spectrum of silica glass. The frequency of the stretching vibration mode increases contrary to that of the rotational modes when the amount of dissolved hydrogen increases at high pressure. Under the isotopic substitution of hydrogen by deuterium, the vibration mode frequency decreases as the square root of D_2/H_2 mass ratio, whereas the rotational mode frequency decreases as a ratio of D_2 to H_2 inertia moments. The rotational modes, overlapped with the phonon modes of silica glass, strengthen unusually at high temperature contrary to the H–H stretching vibration and silica glass modes. The changes in the frequencies of hydrogen phonon modes are irreversible with temperature and refer to hydrogen losses under heating. The molecules of hydrogen gas in the voids of silica glass rotate freely; however, their rotation may be somewhat inhibited due to the van der Waals interaction with the "fixed" atoms of silica glass. A decrease in the frequency of rotational modes associated with the inhibition of rotations exceeds an anticipated increase related to the pressure-induced contraction of the H-H bond. The amount of loosed hydrogen under heating can be determined from a change in the relative intensity of rotational modes with respect to the full intensity of silica glass phonons. The time-dependent changes in the Raman spectra of hydrogenated silica glass upon annealing at an elevated temperature can provide information on the kinetics of hydrogen desorption and may be used to define the activation energy of hydrogen release.

Declaration of competing interest

The authors declare that they have no known competing financial interests or personal relationships that could have appeared to influence the work reported in this paper.

Acknowledgments

REFERENCES

[1] Durbin DJ, Malardier-Jugroot C. Review of hydrogen storage techniques for on board vehicle applications. Int J Hydrogen Energy 2013;38:14595–617. https://doi.org/10.1016/j.ijhhydene.2013.07.-58.

[2] Jena P. Materials for hydrogen storage: past, present, and future. J Phys Chem Lett 2011;2:206e11. https://doi.org/10.1021/jz1015372.

[3] Yartys VA, Lototskyy MV, Akiba E, Albert R, Antonov VE, Ares JR, Baricco M, Bourgeois N, Buckley CE, et al. Magnesium based materials for hydrogen based energy storage: past, present and future. Int J Hydrogen Energy 2019;44:7809–59. https://doi.org/10.1016/j.ijhhydene.2018.12.212.

[4] Iwase Kenji, Mori Kazuhiro. Crystal structure of intermetallic compound Y5Co19 and its hydride phases. Int J Hydrogen Energy 2021;46:9142–50. https://doi.org/10.1016/j.ijhhydene.2021.01.25.

[5] Meletov KP, Maksimov AA, Tartakovskii II, Bashkin IO, Shestakov VV, Krestinin AV, YuM Shulga, Andrikopoulos K, Arvanitidis Y, Christifilos D, Kourouklis GA. Raman study of the high-pressure hydrogenated SWNT: in search of chemically bonded and adsorbed molecular hydrogen. Chem Phys Lett 2007;433:335–9. https://doi.org/10.1016/j.cplett.2006.11.072.

[6] Strobel Timothy A, Sloan ED, Koh CA, Huq A, Schultz AJ. Molecular hydrogen occupancy in binary THF–H_2 clathrate hydrates by high resolution neutron diffraction. J Phys Chem B 2006;110(29):14024–7. https://doi.org/10.1021/jp063164w.

[7] Lokshin KA, Zhao Yusheng. Fast synthesis method and phase diagram of hydrogen clathrate hydrate. Appl Phys Lett 2006;88:131909–1–131909–3. https://doi.org/10.1063/1.2190273.

[8] Hartwig ChM. Raman scattering from hydrogen and deuterium dissolved in silica as a function of pressure. J Appl Phys 1976;47:956–9. https://doi.org/10.1063/1.322686.

[9] Efimchenko VS, Fedotov VK, Kuzovnikov MA, Zhuravlev AS, Bulychev BM. Hydrogen solubility in amorphous silica at pressures up to 75 kbar. J Phys Chem B 2013;117:422–5. https://doi.org/10.1021/jp309991x.

[10] Efimchenko VS, Fedotov VK, Kuzovnikov MA, Meletov KP, Bulychev BM. Hydrogen solubility in cristobalite at high pressure. J Phys Chem 2014;118:10268–72. https://doi.org/10.1021/jp509470q.

[11] Efimchenko VS, Barkovskii NV, Fedotov VK, Meletov KP. Hydrogen solubility in amorphous Mg0.6SiO2.6 at high

pressure. J Exp Theor Phys Lett 2017;124:914–9. https://doi.org/10.1134/S1063776117050028.

[12] Efimchenko VS, Barkovskii NV, Fedotov VK, Meletov KP, Simonov SV, Khasanov SS, Khryapin KI. High-pressure solid solutions of molecular hydrogen in amorphous magnesium silicates. J Alloys Compd 2019;770:229–35. https://doi.org/10.1016/j.jallcom.2018.08.111.

[13] Efimchenko VS, Barkovskii NV, Fedotov VK, Meletov KP, Chernyak VM, Khryapin KI. Destruction of fayalite and formation of iron and iron hydride at high hydrogen pressures. Phys Chem Miner 2019;46:743–9. https://doi.org/10.1007/s00269-019-01035-z.

[14] McLennan JC, McLeod JH. The Raman effect with liquid oxygen, nitrogen, and hydrogen. Nature 1929;123:160. https://doi.org/10.1038/123160a0.

[15] Allin EJ, Feldman T, Welsh HL. Raman spectra of liquid and solid hydrogen. J Chem Phys 1956;24:1116–7. https://doi.org/10.1063/1.1742711.

[16] Allin EJ, McKague AH, Soots V, Welsh HL. The Raman spectrum of solid hydrogen. J Phys 1965;26:615–20. https://doi.org/10.1051/jphys:019650026011061500.

[17] Ashcroft NW. Metallic hydrogen: a high-temperature superconductor? Phys Rev Lett 1968;21:1748–9. https://doi.org/10.1103/PhysRevLett.21.1748.

[18] Sharma K, Mao HK, Bell PM. Raman measurements of hydrogen in the pressure range 0.2-630 kbar at room temperature. Phys Rev Lett 1980;44:886–8. https://doi.org/10.1103/PhysRevLett.44.886.

[19] Mao HK, Hemley RJ. Ultrahigh-pressure transitions in solid hydrogen. Rev Mod Phys 1994;66:671–2. https://doi.org/10.1103/RevModPhys.66.671.

[20] Huang Xiaomi, Li Fangfei, Huang Yanping, Wu Gang, Li Xin, Zhou Qiang, Liu Bingbing, Cui Tian. High-pressure Raman study of solid hydrogen up to 300 GPa. Chin Phys B 2016;25. https://doi.org/10.1088/1674-1056/25/3/037401. 037401-1-5.

[21] Giannasi A, Celli M, Uilvi L, Zoppi M. Low temperature Raman spectra of hydrogen in simple and binary clathrate hydrates. J Chem Phys 2008;129:084705. https://doi.org/10.1063/1.2971185. 1-10.

[22] Giannasi A, Celli M, Zoppi M, Moraldi M, Uilvi L. Experimental and theoretical analysis of the rotational Raman spectrum of hydrogen molecules in clathrate hydrates. J Chem Phys 2011;135:054506-1–054506-9. https://doi.org/10.1063/1.3618549.

[23] Strobel TA, Sloan ED, Koh CA. Raman spectroscopic studies of hydrogen clathrate hydrates. J Chem Phys 2009;130:014506. https://doi.org/10.1063/1.3046678.

[24] Khvostantsev LG, Slesarev VN, Brazhkin VV. Toroid type high-pressure device: history and prospects. High Press Res 2004;24:371–83. https://doi.org/10.1080/08957950412331298761.

[25] Antonov VE, Bashkin IO, Khasanov SS, Moravsky AP, Morozov YuG, YuM Shulga, Ossipyan YuA, Ponyatovsky EG.

Magnetic ordering in hydrofullerite $C_{60}H_{24}$. J Alloys Compd 2002;330–332:365–8. https://doi.org/10.1016/S0925-8388(01)01534-1.

[26] Antonov VE, Bulychev BM, Fedotov VK, Kapustin DI, Kulakov VI, Sholin IA. NH_3BH_3 as an internal hydrogen source for high pressure experiments. Int J Hydrogen Energy 2017;42:22454–9. https://doi.org/10.1016/j.ijhydene.2017.03.121.

[27] Bashkin IO, Antonov VE, Bazhenov AV, Bdikin IA, Borisenko DN, et al. Thermally stable hydrogen compounds obtained under high pressure on the basis of carbon nanotubes and nanofibers. JETP Lett (Engl Transl) 2004;79:226–30. https://doi.org/10.1134/1.1753421.

[28] Meletov KP. A nitrogen cryostat with adjustable temperature and cold loading of samples for the measurement of optical spectra. Instrum Exp Tech 2020;63:291–3. https://doi.org/10.1134/S0020441220020013.

[29] Chrissanthopoulos A, Bouropoulos N, Yannopoulos SN. Vibrational spectroscopic and computational studies of sol-gel derived $CaO-MgO-SiO_2$ binary and ternary bioactive glasses. Vib Spectrosc 2008;48:118–25. https://doi.org/10.1016/j.vibspec.2007.11.008.

[30] Enkovich PV, Brazhkin VV, Lyapin SG, Kanda H, Novikov AP, Stishov SM. Quantum effects in diamond isotopes at high pressures. Phys Rev B 2016;93:014308-1–014308-4. https://doi.org/10.1103/PhysRevB.93.014308.

[31] Landau LD, Lifshitz EM. Quantum mechanics: non-relativistic theory. 3rd ed. New York: Pergamon; 1977.

[32] England W, Raich JC, Etters RD. Rotational motion under pressure in the solid molecular hydrogen isotopes. J Low Temp Phys 1976;22:213–22. https://doi.org/10.1007/BF00655222.

[33] Subramanian S, Sloan ED. Trends in vibrational frequencies of guests trapped in clathrate hydrate cages. J Phys Chem B 2002;106:4348–55. https://doi.org/10.1021/jp013644h.

[34] Plotnichenko VG, Vasiliev SA, Rybaltovskii AO, Koltashev VV, Sokolov VO, Klyamkin SN, Medvedkov OI, Rybaltovskii AA, Malosiev AR, Dianov EM. Hydrogen diffusion and ortho–para conversion in absorption and Raman spectra of germanosilicate optical fiber hydrogen-loaded at 150–170 MPa. J Non-Cryst Solids 2005;351:3677–84. https://doi.org/10.1016/j.jnoncrysol.2005.10.004.

[35] Pimentel GC, Charles SW. Infrared spectral perturbations in matrix experiments. Pure Appl Chem 1963;7:111–23. https://doi.org/10.1351/pac196307010111.

[36] Hirai H, Ohno S, Kawamura T, Yamamoto Y, Yagi T. Changes in vibration modes of hydrogen and water molecules and in lattice parameters with pressure for filled-ice hydrogen hydrates. J Phys Chem C 2007;111:312–5. https://doi.org/10.1021/jp064281u.